Open source algorithms for maximizing V2G flexibility based on model predictive control

Diaz-Londono, Cesar; Orfanoudakis, Stavros; Vergara Barrios, P.P.; Palensky, P.; Ruiz, Fredy ; Gruosso, Giambattista

DOI
10.1016/j.epsr.2025.112082

Publication date
2026

Document Version
Final published version

Published in
Electric Power Systems Research

Electric Power Systems Research 250 (2026) 112082

Contents lists available at ScienceDirect

Electric Power Systems Research

journal homepage: www.elsevier.com/locate/epsr

Open source algorithms for maximizing V2G flexibility based on model predictive control

Cesar Diaz-Londono [a,b], Stavros Orfanoudakis [c,*], Pedro P. Vergara [c], Peter Palensky [c], Fredy Ruiz [b], Giambattista Gruosso [b]

[a] Center for Research on Microgrids (CROM), Huanjiang Laboratory, Wenzhong Road No. 7, Zhuji, Shaoxing, Zhejiang, 311800, China
[b] Politecnico di Milano, Dipartimento di Elettronica, Informazione e Bioingegneria, Via G. Ponzio, Milan, 20133, Milano (MI), Italy
[c] Delft University of Technology, Intelligent Electrical Power Grids, Mekelweg 5, Delft, 2628 CD, The Netherlands

ARTICLE INFO

Keywords:
Electric vehicles (EVs)
Smart charging
Battery degradation
Vehicle-to-Grid (V2G)
Model predictive control (MPC)

ABSTRACT

Integrating electric vehicles (EVs) into the power grid can revolutionize energy management strategies, offering both challenges and opportunities for creating a more sustainable and resilient grid. In this context, model predictive control (MPC) emerges as a powerful tool for addressing the complexities of Grid-to-Vehicle (G2V) and Vehicle-to-Grid (V2G) enabled demand response management. By leveraging advanced optimization techniques, MPC algorithms can anticipate future grid conditions and dynamically adjust EV charging and discharging schedules. However, no standard tools exist to evaluate novel energy management strategies based on MPC approaches. This work focuses on harnessing the potential of MPC in G2V and V2G applications by providing open-source algorithms that allow the maximization of EV flexibility and support demand response initiatives while mitigating the impact on EV battery health. Through extensive simulation and analysis, we demonstrate the efficacy of our approach in maximizing the benefits of G2V and V2G while assessing the impact on the longevity and reliability of EV batteries. Specifically, the proposed methods enable the optimization of EV charging and discharging schedules in real-time, taking into account fluctuating energy prices, grid constraints, and EV user preferences.

1. Introduction

As the adoption of electric vehicles (EVs) continues to surge, the efficient management of charging infrastructure becomes increasingly important [1]. Grid-to-vehicle (G2V) technology facilitates energy flow in a unidirectional manner, whereas vehicle-to-grid (V2G) technology enables bidirectional energy flow between EVs and the grid, thereby unlocking the potential for EV batteries to serve as flexible energy storage resources [2,3]. However, the effective implementation of G2V and V2G strategies faces numerous uncertainties, including fluctuating energy demands, variable renewable energy generation, inflexible loads, and dynamic EV schedules [4].

1.1. Literature review

Various strategies have been explored in the literature to address the EV smart charging problem, aiming to balance user requirements, grid stability, and energy cost optimization. Among them, rule-based approaches have been widely adopted due to their practical simplicity and effectiveness. One example is the strategy presented in [5], which incorporates V2G integration, allowing EVs to inject power back into the grid during peak-load or high-tariff periods. A similar rule-based framework is described in [6], where both charging and discharging processes are managed in the context of renewable energy systems to enhance grid flexibility. Literature review Table 1 provides a comprehensive comparison of key algorithmic approaches for smart EV charging, highlighting their capabilities in terms of real-time operation, V2G support, battery degradation modeling, open-source availability, and benchmarking against optimal solutions.

To address the increasing complexity of smart charging scenarios, heuristic and metaheuristic methods have also been explored. A fuzzy logic-based control system for managing EV battery charging and discharging is proposed in [7], offering adaptive responses under varying grid conditions. In [8], an improved honey badger algorithm, combined with dynamic programming, is employed to optimize G2V and V2G power flows in a system that integrates EV parking lots. Additionally, the artificial bee colony optimization algorithm described in [9] addresses the multi-objective optimization challenges inherent in smart charging, drawing inspiration from the foraging behavior of

* Corresponding author.
E-mail address: s.orfanoudakis@tudelft.nl (S. Orfanoudakis).

https://doi.org/10.1016/j.epsr.2025.112082
Received 26 July 2024; Received in revised form 23 July 2025; Accepted 29 July 2025
Available online 20 August 2025

Notation

Sets and Indices

I	Set of EV chargers, indexed by i
J	Set of EVs, indexed by j
G	Set of transformers, indexed by g
K	Set of time steps, indexed by k
H	MPC prediction horizon, indexed by h
Φ_g	Chargers connected to transformer g

Parameters

Δt	Time step duration
E_j	Battery capacity of EV j
a_j, d_j	Arrival and departure time of EV j
$\overline{P}_i^c$, $\overline{P}_i^d$	Max charging/discharging power at charger i
η^c, η^d	Charging/discharging efficiency
π_k^c, π_k^d	Charge/discharge price at time k
$\pi_{k,Flex}^c$, $\pi_{k,Flex}^d$	Flexibility prices at time k
SoC_{j,a_j}	SoC at EV arrival
$\underline{SoC}_{j,d_j}$, $\overline{SoC}_{j,d_j}$	Min and max target SoC at EV departure
$SoC_{j,\min}$	Minimum SoC allowed while discharging
$\underline{x}_{i,k}$, $\overline{x}_{i,k}$	Min and max battery capacity
Ψ_g	Transformer power limit
$\tilde{l}_{g,k}$, $\tilde{w}_{g,k}$	Forecasted load/PV gen. at transformer g
$P_{g,k}^{DR}$	Demand Response power at transformer g

Decision Variables

$P_{i,k}^c$, $P_{i,k}^d$	Ch. & disch. power at charger i and time k
$z_{i,k}$	Binary: 1 for charging, 0 for discharging
$x_{i,k}$	Battery capacity of the EV at charger i and time k
$F_{i,k}^c$, $F_{i,k}^d$	Offered charging/discharging flexibility

Other Variables

$\xi_{i,k}$	EV connection status at charger i and time k
O_k^{CM}	Operating cost at time k
O_k^{FM}	Flexibility reward at time k
Q^{lost}	Total battery capacity lost
d^{cal}, d^{cyc}	Calendar/cyclic battery degradation

honeybees. Other metaheuristic techniques, such as particle swarm optimization and genetic algorithms, have also demonstrated promising results in reducing fluctuations during bidirectional charging, as discussed in [10].

Reinforcement Learning (RL) methods have further contributed to the development of intelligent and adaptive charging strategies [11,12]. In particular, real-time energy management systems based on RL have shown the potential to achieve significant energy savings in EV integration scenarios [13]. Complementarily, consensus-based algorithms combined with blockchain principles have been proposed to coordinate EV charging with low computational complexity, as presented in [14].

Other approaches rely on mathematical programming techniques to address the smart charging problem from a formal optimization perspective. For instance, in [15], a real-time approach is introduced to manage EV charging schedules using satisfaction assignment and prioritized charging strategies, all while considering operational constraints. Additionally, in [16], a linear model is employed to maximize the utilization of photovoltaic (PV) power generation during EV charging peaks, while ensuring the EVs' state of charge (SoC) constraints are met. Furthermore, Linear Programming (LP) techniques have been utilized to optimize load factor during daily operations of EV parking lots, considering uncertainties in EV behavior such as arrival and departure times [17]. Similarly, [18] proposes a mixed-integer programming model to maximize revenues for a V2G EV aggregator in the UK electricity market. In [19], the synchronization of forecast-based optimization with management operation is implemented for EV charging and discharging patterns. Optimal dispatching methods can reduce the curtailment of wind turbines and PV power [20] or reduce the generation cost [21] in distribution systems. While these approaches provide linear models for both small and large-scale problems, they are limited due to the absence of real-time control to handle the inherent uncertainties.

Model Predictive Control (MPC) stands out as a powerful solution for navigating the intricacies of G2V and V2G-enabled demand response management [22]. In [23], a real-time MPC strategy was proposed, effectively reducing operational costs by treating EVs as flexible loads, thereby enabling adjustments in the power allocation and charging duration for each EV. Similarly, in [24], an MPC method was introduced to coordinate EVs on a large scale, enhancing grid robustness and cutting operational expenses. Moreover, [25] proposed a scenario-based MPC approach, combining robust and stochastic models to minimize the total operational cost for energy management. In [26], a real-time cost-minimization energy management strategy was introduced, aiming to maximize the economic potential of EVs while addressing battery degradation, thus mitigating a single vehicle's operating costs. Beyond economic optimization, MPC has also been recognized for its ability to contribute to grid stability. For instance, advancements in MPC have shown effectiveness in mitigating frequency fluctuations and reducing harmonic distortions, making it a viable solution for maintaining power system stability in renewable-dominated grids [27]. Additionally, MPC has demonstrated potential in delivering ancillary services such as frequency containment reserve, further supporting its role in modern grid management [28]. Even though many MPC methods have been developed, there remains a gap in achieving a comprehensive real-time demand response solution while assessing battery degradation.

Furthermore, while there are many open-source simulation tools for fleet charging management, they often lack baseline MPC implementations. For instance, FleetRL [29] provides a customizable environment for commercial vehicle fleets, utilizing RL for charging optimization, assessing factors like economic feasibility, battery health, and operational efficiency. While FleetRL offers a useful simulation framework, it lacks support for constraint-aware optimization and does not incorporate MPC-based coordination for flexibility or battery health. Similarly, Chargym [30] and SustainGym [31] offer simulation environments for EV charging, focusing on RL algorithm development but with simplified models. Other platforms also illustrate this limitation. OPEN [32] addresses broader smart energy systems but lacks MPC integration. The Open V2X Management Platform [33] emphasizes clustering EV users into behavioral profiles and forecasting daily energy demand at charging stations; it does not integrate any MPC-based control mechanism. Likewise, the tool introduced in [34] enables advanced V2G analysis within urban power and transportation networks. Still, coordination is based on participation willingness rather than optimal dispatch, limiting its applicability for optimization-based strategies. In [35], a real-time charging heuristic is proposed to maximize driver satisfaction and ensure fair power allocation; however, it does not leverage predictive control methods such as MPC. Considering the demonstrated effectiveness of MPC in EV smart charging, the development of an open-source MPC-based framework is critically important. Such a platform would enable standardized benchmarking, foster reproducible research, and facilitate the practical evaluation of MPC strategies under realistic operational constraints, ultimately bridging the gap between academic research and real-world deployment.

Table 1
Literature review table for Smart EV Charging approaches.

References	Algorithm	Approach	Real-time	V2G	Battery degradation	Open-source	Compared with optimal solution
[6]	PSO, GA, etc.	Metaheuristic	Yes	Yes	No	No	No
[7]	Fuzzy logic	Hybrid	Yes	Yes	No	No	No
[8]	Honey badger	Metaheuristic	No	Yes	No	No	No
[9]	Bee colony	Metaheuristic	No	No	No	No	No
[10]	PSO, GA	Metaheuristic	No	Yes	No	No	No
[11,12]	Reinforcement learning	Learning-based	Yes	Yes	No	Yes	Yes
[14]	Consensus-based blockchain	Distributed	Yes	Yes	No	No	No
[16,17]	Linear optimization	Mathematical Prog.	No	No	No	No	Yes
[18,19]	Mixed-integer LP	Mathematical Prog.	No	Yes	No	No	Yes
[15]	Real-time satisfaction assignment	Mathematical Prog.	Yes	No	No	No	Yes
[23–25]	Real-Time MPC	MPC	Yes	No	No	No	Yes
[26]	Cost-minimization MPC	MPC	Yes	Partial	Yes	No	Yes
[27,28]	Frequency regulation MPC	MPC	Yes	Partial	No	No	No
[29]	FleetRL	RL simulator	Yes	Yes	Yes	Yes	No
[30,31]	Chargym, SustainGym	RL simulator	Yes	Partial	No	Yes	No
[32]	OPEN platform	General simulation	Yes	No	No	Yes	Yes
[33–35]	Open V2X	Simulation framework	Yes	No	No	Yes	No
This work	**Proposed MPC framework**	MPC	Yes	Yes	Yes	Yes	Yes

1.2. Article contributions

To bridge the identified gaps, this work presents a fully open-source implementation of MPC algorithms for smart EV charging and discharging.[1] The framework is designed to maximize the profit of CPOs, while incorporating user preferences and accounting for key uncertainties such as inflexible loads, photovoltaic generation, and demand response events. In addition to the software release, a complete mathematical formulation of the underlying optimization problem is provided, ensuring full transparency and reproducibility. To the best of the authors' knowledge (as shown in Table 1), this is the first openly available open-source MPC framework specifically tailored to the EV smart charging context. Its performance is assessed through comprehensive simulations and is benchmarked against representative rule-based approaches and RL strategies. In summary, the main contributions of this study are:

- Development of flexible open-source MPC algorithms capable of executing various EV CPO case studies to evaluate different performance indicators.
- Novel formulation of an economic MPC method tailored for G2V and V2G real-time smart charging, strategically crafted to optimize profits while accommodating uncertainties intrinsic to demand response.
- Capable of handling EVs and charging stations with heterogeneous characteristics.
- Innovative design of the Optimal control with maximum flexibility (OCMF) MPC method for G2V and V2G real-time smart charging, geared towards enhancing flexibility and profitability amidst the complexities of demand response uncertainties.
- Evaluation of the impact of smart charging strategies on the degradation of EV batteries.

1.3. Article organization

The structure of the article is as follows. Section 2 outlines the background and fundamental aspects of the EV charging management problem. This is followed by an in-depth presentation of smart charging strategies and their mathematical formulations in Section 3. The experimental setup used to evaluate the proposed methods is detailed in Section 4. A comprehensive evaluation and comparison with baseline strategies are presented in Section 5 to demonstrate the effectiveness of the proposed approaches. In Section 6, conclusions and potential future research directions are discussed.

[1] Access the open-source code at https://github.com/CesarDiazLondono/MPC-G2V-V2G and https://github.com/StavrosOrf/EV2Gym.

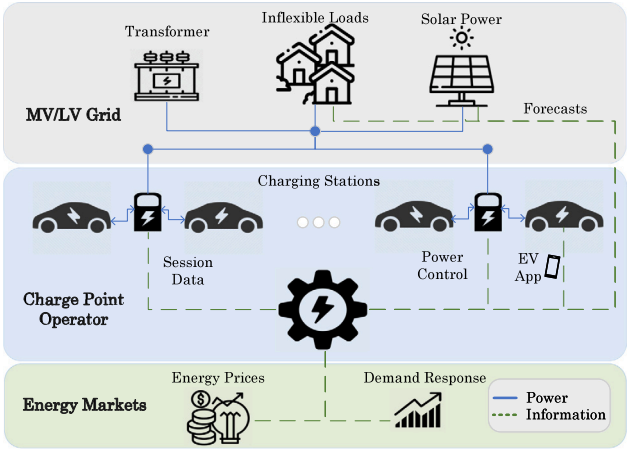

Fig. 1. Overview of the EV charging management system, illustrating power and information flows between the distribution grid, inflexible household loads, PV, transformer, charging infrastructure, and energy markets. The CPO in the middle processes signals from the market, distribution grid, and EV users in order to efficiently control the connected EVs.

2. EV charging management

In this section, an overview of the EV charging problem and the simulation tool used is provided. Specifically, a comprehensive simulator platform for conducting realistic V2G simulations is discussed. This platform encompasses configurable simulation parameters, realistic EV models, efficient charging station management, and detailed transformer operations.

2.1. Simulation models

In a simulation, there are I chargers, where $i = 1, 2, \dots, I$, each one having one Electric Vehicle Supply Equipment (EVSE). Each charger i is connected to one of the G transformers, where $g = 1, 2, \dots, G$. There are also, J EVs that connect to EVSEs during the simulation. Finally, a simulation consists of K discrete time steps, where $k = 1, 2, \dots, K$. At each step, the user-selected algorithm defines the power output $P_{i,k}$, for each charger i. The algorithm can fully observe the current state of the environment and can access future data, including electricity prices, load and PV forecasts, and EV schedules. Fig. 1 illustrates the simulator models.

Each EV j in the simulator features customizable parameters, including battery capacity (E_j), charge (η^c) and discharge (η^d) efficiency,

Table 2
Battery degradation model parameters.

ϵ_0	ϵ_1	ϵ_2	θ	ζ_0	ζ_1	K^{tot}	Q^{acc}
$6.23 \cdot 10^6$	$1.38 \cdot 10^6$	6976	28	$4.02 \cdot 10^{-4}$	$2.04 \cdot 10^{-3}$	730	11 160

minimum SoC at departure $\underline{\text{SoC}}_{j,d_j}$, and maximum charging ($\overline{P}_i^c$) and discharging ($\overline{P}_i^d$) power limits that depend not only on the EV battery management system but also on the EVSE rated power. In our use case, EV users communicate their expected arrival and departure times, along with an estimate of their SoC upon arrival. This information enables the CPO to make more informed scheduling decisions, improving the coordination and utilization of the available charging infrastructure across the EV fleet. At each time step k EVs can arrive at a charging station based on realistic EV behavior probability distributions obtained from the ElaadNL repository [36], ensuring the simulation accurately reflects real-world scenarios. Therefore, an EV's arrival time a_j, departure time d_j, and SoC at arrival SoC_{a_j} are sampled from ElaadNL data. By leveraging this data, the simulator can replicate various charging patterns observed in different settings, such as public charging stations, workplaces, and residential areas.

Each transformer g aggregates EV chargers in the set Φ_g, to simulate the electricity distribution network and its constraints. Additionally, transformers incorporate realistic data about inflexible loads, solar photovoltaic (PV) generation, and demand response (DR) events. For instance, datasets from Pecan Street [37] and Renewables.ninja [38] are used to model inflexible loads and PV generation profiles, respectively, while information about demand response events can be configured by users based on specific parameters such as start time and duration. Transformers have operational constraints that must be followed. Violations of these constraints are tracked throughout the simulation, enabling the evaluation of charging strategies under realistic operating conditions. Furthermore, the platform generates forecasts of inflexible loads and solar power generation to support the development of algorithms that can handle uncertainty, enhancing the robustness and reliability of charging strategies in real-world scenarios.

DR mechanisms are also supported within the simulation platform. These can be implemented through various contractual arrangements between EV owners, the CPO, and the system operator. For example, the framework proposed in [39] introduces a three-stage process: (i) quantifying the potential profit that EV owners can achieve based on their flexibility, (ii) establishing DR contracts between the CPO and EV owners accordingly, and (iii) defining the profit and penalty sharing mechanisms among stakeholders. In the present work, we assume that such contractual agreements are predefined and established before the simulation starts. Therefore, the negotiation and formation of DR contracts are considered out of the scope of this study. Instead, these agreements are treated as fixed inputs provided to the CPO. The algorithm implemented by the CPO can identify EVs with available flexibility for DR participation.

2.2. Battery degradation model

Users often hesitate to offer their EVs for V2G services due to concerns about battery degradation. For this reason, it is important to assess the impact of the proposed smart charging algorithms using a validated battery degradation model [40]. This model comprises both calendar (d^{cal}) and cyclic (d^{cyc}) capacity loss components. For a single EV, based on [40], the capacity degradation attributed to calendar aging over a simulation with duration K is related to the mean $\widehat{\text{SoC}}$ and is described as:

$$d^{cal} = 0.75 \cdot (\epsilon_0 \cdot \widehat{\text{SoC}} - \epsilon_1) \cdot \exp\left(-\frac{\epsilon_2}{\theta}\right) \cdot \frac{K}{(K^{tot})^{0.25}}. \quad (1)$$

Here, K^{tot} denotes the battery's age in days, θ represents the battery temperature (°C), and $\epsilon_0, \epsilon_1, \epsilon_2$ are constants, as shown in Table 2.

The cyclic capacity loss depends on the total energy exchanged by the battery and the SoC at each simulation step as:

$$d^{cyc} = \left(\zeta_0 + \zeta_1 \frac{\sum |\widehat{\text{SoC}} - \text{SoC}_k| \, \Delta t}{K}\right) \cdot \frac{\sum |P_k| \, \Delta t}{\sqrt{Q^{acc}}}, \quad (2)$$

where Q^{acc} is the accumulated throughput during the battery's lifetime, and ζ_0, ζ_1 are constants defined in Table 2. Therefore, the total capacity loss of an EV battery is the sum: $Q^{lost} = d^{cal} + d^{cyc}$. In this work, the capacity loss is evaluated but not included in the vehicle model within the charging strategies presented in the next section.

3. Smart charging strategies

The smart charging strategies adopted by the CPO rely on the MPC algorithm. The proposed strategies are based on [41], in which only unidirectional strategies are considered. In this paper, we are proposing four distinct smart charging algorithms, each designed to achieve specific objectives while adhering to the MPC framework. These strategies include:

- eMPC G2V: Unidirectional economic MPC (eMPC) aimed at minimizing the operational costs of the CPO.
- eMPC V2G: Bidirectional eMPC aimed at minimizing the operational costs of the CPO.
- OCMF G2V: Unidirectional Optimal Control with Maximum Flexibility (OCMF) aimed at minimizing the CPO's operational costs while maximizing charger flexibility.
- OCMF V2G: Bidirectional OCMF aimed at minimizing the CPO's operational costs while maximizing charger flexibility.

3.1. Solution formulation

The proposed MPC algorithms are designed to maximize CPO profits, taking into consideration constrains on energy and power limits imposed by the grid, chargers and vehicles, the preferences of EV owners and the various uncertainties associated with the charging pool, such as the inflexible loads and the PV generation. MPC algorithm forms the basis of this approach, where at each time step k, an optimization program is solved to determine the optimal power exchange between each charger in the pool I with an EV connected, and the grid for an horizon of H steps. Then, the algorithm outputs are the demanded and delivered charger power levels for the current time step k, denoted as $P_{i,k}^{c*}$ and $P_{i,k}^{d*}$, respectively. Notice that only one of these power levels can be activated for every charger at each interval k, i.e., the charger can only charge or discharge the EV at k. On the other hand, the plant under control is the set of EVs connected to the chargers. Power commands $P_{i,k}^{c*}$ and $P_{i,k}^{d*}$ are the inputs to the actual EV charging pool, where the SoC of the vehicles' batteries, represented as $x_{i,k}$, are the system state and model outputs.

The MPC methodology involves four main steps:

1. Given the SoC of the connected vehicles at time k, build a prediction model to compute the evolution of the SoC of the EV charging pool $x_{i,k+h}$ over a prediction horizon H for any power profiles $P_{i,k+h}^{c}$ and $P_{i,k+h}^{d}$, where $h = 1, 2, \ldots, H$.
2. Optimization process to determine the future inputs $P_{i,k+h}^{c*}$ and $P_{i,k+h}^{d*}$, considering a cost function and operational constraints.
3. Application of the first element of the optimal power profile $P_{i,k}^{c*}$ or $P_{i,k}^{d*}$ (h=0) to the chargers within the pool.
4. Wait until the next time step to measure the new system state $x_{i,k+1}$ and forecasted variables, such as the inflexible loads and the PV generation.

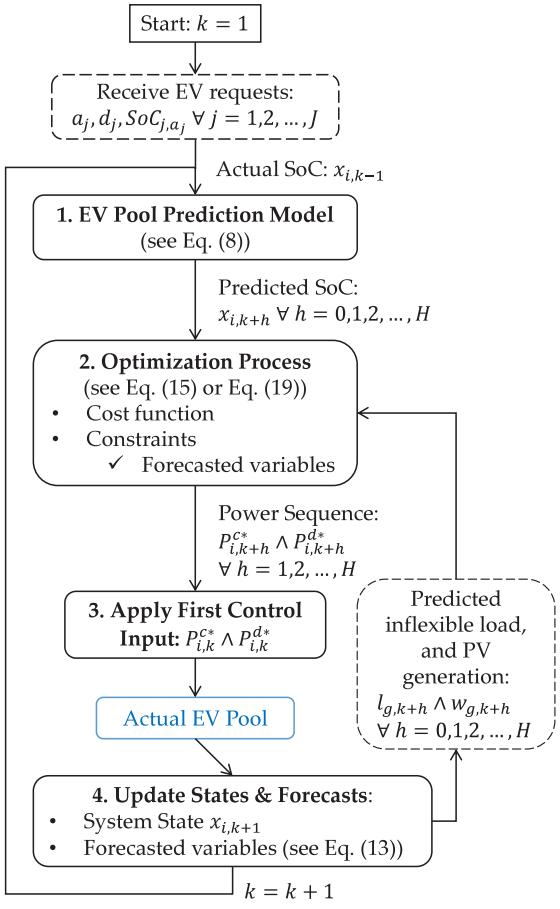

Fig. 2. Flowchart of the MPC algorithm methodology.

These steps are iterated at each time step k, employing the concept of receding horizon. This approach involves recalculating the power signals $P^{c*}_{i,k}$ and $P^{d*}_{i,k}$ at each iteration, taking into account updated information. This methodology is illustrated in the flowchart shown in Fig. 2. The process begins at $k = 1$, upon receiving all EV charging requests, which could, for instance, be submitted through an application by the EV owner. The four main steps of the control strategy are then executed sequentially. It is important to note that the predicted inflexible load and PV generation are updated at every time step k, and these updated forecasts are incorporated when solving the optimization problem. Although the prediction of inflexible load and PV generation is not the focus of this paper, they are treated as exogenous inputs to the control algorithm. While the accuracy of these forecasts impacts the MPC's performance, its iterative closed-loop nature helps mitigate uncertainty through continuous feedback operation, as illustrated in [42]. In practice, such forecasts can be obtained from a neural network model running in parallel to the control loop, which updates its predictions whenever a new measurement becomes available. The equations referenced in the flowchart are presented later in the paper.

The MPC algorithm relies on a system model to predict future powers in the charging pool. Therefore, this model must strike a balance between precision, to factor in charger responses, and simplicity, to facilitate online optimization for the Real-Time (RT) operation of the chargers. Hence, the EV charger model depends on a signal $\xi_{i,k}$ indicating whether an EV is plugged in at the kth time slot, along with the SoC variation of the plugged-in EV. The signal $\xi_{i,k}$ is a binary variable, $\xi_{i,k} = 1$ if the charger i has a plugged-in EV.

The SoC evolution on the jth EV plugged-in the charger i (i.e., $\xi_{i,k} = 1$) is:

$$x_{i,k+1} = x_{i,k} + \frac{\Delta t}{E_j}\left(\eta^c P^c_{i,k} - \frac{P^d_{i,k}}{\eta^d}\right), \tag{3}$$

while the state space model for an EV charging pool considers three possible conditions, as:

$$x_{i,k+1} = \begin{cases} \mathrm{SoC}_{j,a_j} & \text{if} \quad k = a_j, \\ \text{Eq. (3)} & \text{if} \quad a_j < k < d_j, \\ 0 & \text{if} \quad \xi_{i,k}{=}0 \vee k{=}d_j. \end{cases} \tag{4}$$

The first condition corresponds to the arrival SoC, denoted as SoC_{j,a_j}. The second condition represents the evolution of the energy stored in the EV battery. The third condition applies when there is no EV connected or when an EV is departing. Note that Eq. (4) applies to the entire pool of I EV chargers, rather than to an individual EV.

Then, the EV charging pool model for the time slot k is defined as:

$$\hat{\mathrm{x}}_{k+1} = A_k \hat{\mathrm{x}}_k + B_k \hat{\mathrm{P}}_k, \tag{5}$$

where, the charging pool outputs, i.e., the SoC in the chargers are presented in the $\hat{\mathrm{x}}_k \in \mathbb{R}^I$, as:

$$\hat{\mathrm{x}}_k = [x_{1,k}\ x_{2,k}\ \dots\ x_{I,k}]^{\mathrm{T}},$$

and the exchanged power pool inputs, i.e., the charging and discharging powers are grouped in one vector denoted $\hat{\mathrm{P}}_k \in \mathbb{R}^{2I}$, as:

$$\hat{\mathrm{P}}_k = [P^c_{1,k}\ P^d_{1,k}\ P^c_{2,k}\ P^d_{2,k}\ \dots\ P^c_{I,k}\ P^d_{I,k}]^{\mathrm{T}}.$$

Moreover, $A_k = \mathrm{diag}(\xi_{i,k})$ containing information about the plugged-in EVs in the chargers, then, $A_k \in \mathbb{R}^{I\times I}$. Considering $b^c_{i,k}$ and $b^d_{i,k}$ as:

$$b^c_{i,k} = \frac{\xi_{i,k}\Delta t \eta^c}{E_j} \quad \wedge \quad b^d_{i,k} = \frac{\xi_{i,k}\Delta t}{E_j \eta^d}, \tag{6}$$

the matrix $B_k \in \mathbb{R}^{I\times 2I}$ is generated as:

$$B_k = \begin{bmatrix} b^c_{1,k} & -b^d_{1,k} & 0 & 0 & \cdots & \cdots & 0 & 0 \\ 0 & 0 & b^c_{2,k} & -b^d_{2,k} & 0 & 0 & 0 & 0 \\ \vdots & \vdots & 0 & 0 & \ddots & \ddots & 0 & 0 \\ 0 & 0 & 0 & 0 & \cdots & \cdots & b^c_{I,k} & -b^d_{I,k} \end{bmatrix}. \tag{7}$$

Note that the model in Eq. (5) accounts for all chargers during time slot k. For the prediction horizon H, the MPC algorithm utilizes the following prediction model.

$$\mathbb{X} = \mathbb{A}\hat{\mathrm{x}}_k + \mathbb{G}\mathbb{P}, \tag{8}$$

where,

$$\mathbb{X} = \begin{bmatrix} \hat{\mathrm{x}}_{k+1} \\ \hat{\mathrm{x}}_{k+2} \\ \vdots \\ \hat{\mathrm{x}}_{k+H} \end{bmatrix}, \quad \mathbb{P} = \begin{bmatrix} \hat{\mathrm{P}}_k \\ \hat{\mathrm{P}}_{k+1} \\ \vdots \\ \hat{\mathrm{P}}_{k+H-1} \end{bmatrix}, \quad \mathbb{A} = \begin{bmatrix} A_k \\ A_k A_{k+1} \\ \vdots \\ A_k \cdots A_{k+H-1} \end{bmatrix},$$
$$\mathbb{G} = \begin{bmatrix} B_k & 0 & 0 & 0 \\ A_{k+1}B_k & B_{k+1} & 0 & 0 \\ \vdots & \vdots & \ddots & 0 \\ A_{k+1}\cdots A_{k+H-1}B_k & A_{k+2}\cdots A_{k+H-1}B_{k+1} & \cdots & B_{k+H-1} \end{bmatrix} \tag{9}$$

The algorithm considers the constraint that the SoC at the departure time d_j of each EV must be within predetermined bounds, i.e., the minimum $\underline{\mathrm{SoC}}_{j,d_j}$ and maximum $\overline{\mathrm{SoC}}_{j,d_j}$ SoC levels specified by the EV owner.

$$\underline{\mathrm{SoC}}_{j,d_j} \le x_{i,d_j} \le \overline{\mathrm{SoC}}_{j,d_j} \tag{10}$$

The SoC in the charger is always positive and depends on the maximum capacity $\overline{x}_i$ of the plugged-in EV battery, as:

$$\underline{x}_{i,k} \le x_{i,k} \le \overline{x}_{i,k}. \tag{11}$$

To avoid deep discharges in the EV battery, a minimum SoC level is defined:

$$\underline{x}_{i,k}=\begin{cases} SoC_{j,a_j} & \text{if } k=a_j, \\ x_{i,k-1} & \text{if } \xi_{i,k}=1 \wedge x_{i,k-1} < SoC_{j,min}, \\ SoC_{j,min} & \text{if } \xi_{i,k}=1 \wedge x_{i,k-1} > SoC_{j,min}, \\ 0 & \text{if } \xi_{i,k}=0. \end{cases} \tag{12}$$

The first condition for the minimum SoC assumes the arrival SoC at the time of arrival. The second and third conditions depend on the minimum state of charge, $SoC_{j,min}$, which represents the threshold at which an EV is allowed to discharge. Consequently, if the actual SoC of the EV is below this threshold, the minimum SoC remains at the actual SoC level until the threshold is reached. Once the threshold is exceeded, the EV battery can be discharged up to the threshold. The final condition applies when no EV is plugged in.

The algorithm is capable of reacting to RT market signals, including fluctuations in price and demand response (DR) events. Specifically, DR requests are represented by the variable P_k^{DR}, allowing the algorithm to promptly respond to market requests as they occur.

The power limit imposed by the each transformer is specified as Ψ_g, then the balance equation for transformer g is constrained as

$$\sum \phi_{g,k} + \tilde{l}_{g,k} - \tilde{w}_{g,k} \leq \Psi_g - P_{g,k}^{DR} \tag{13}$$

where the net power consumed/supplied by the chargers connected to transformer g is $\phi_{g,k} = P_{i,k}^c - P_{i,k}^d, \forall i \in \Phi_g$, and Φ_g denotes the set of EV chargers connected to cluster g. $\tilde{l}_{g,k}$ is the predicted inflexible load, $\tilde{w}_{g,k}$ is the predicted PV generation and $P_{g,k}^{DR}$ is the demand response command is case of a market request.

In the following subsections, the MPC algorithms followed by the EV CPO are presented.

3.2. eMPC: EV CPO cost minimization

This strategy, known as eMPC, seeks to minimize the operational costs of the CPO for the horizon H, by optimizing the EV charging profiles of the pool the interval $[k,\ k+H]$. The algorithm's decisions rely on the RT energy prices π_k^c and π_k^d for charging and discharging, respectively. Therefore, the cost function for V2G in eMPC is formulated as follows:

$$O_k^{CM} = \pi_k^c \sum_{i=1}^{I} P_{i,k}^c - \pi_k^d \sum_{i=1}^{I} P_{i,k}^d \tag{14}$$

Then, the EV CPO deals with the following eMPC V2G problem:

$$\min_{P_{i,k}^c, P_{i,k}^d, z_{i,k}} \quad \Delta t \sum_{k=0}^{H-1} O_k^{CM} \tag{15a}$$

$$\begin{aligned} \text{s.t. Eqs. (4), (10), (11), (13)} \\ 0 \leq P_{i,k}^c \leq \overline{P}_i^c z_{i,k} \\ 0 \leq P_{i,k}^d \leq \overline{P}_i^d (1 - z_{i,k}) \\ \forall\ k = 1,2,\ldots,H,\ i = 1,2,\ldots,I, \\ j = 1,2,\ldots,J,\ g = 1,2,\ldots,G. \end{aligned} \tag{15b}$$

The decision variables of the problem include the charging ($P_{i,k}^c$) and discharging ($P_{i,k}^d$) power profiles, and the binary variables $z_{i,k}$, which determines whether charging or discharging is performed during time slot k. Both the charging and discharging powers are constrained to be between zero and their respective maximum powers, denoted as $\overline{P}_i^c$ and $\overline{P}_i^d$, respectively. Note that problem (15a) is a Mixed-Integer Linear Program (MILP), for which efficient solvers are available.

Notice that this eMPC problem also applies to the G2V strategy, with the only difference being the absence of the remuneration price π_k^d since $P_{i,k}^d$ is always zero. Similarly, the binary variable $z_{i,k}$ is not required, resulting in a much simpler Linear Program (LP), with fewer decision variables.

3.3. OCMF: CPO flexibility maximization

This strategy denoted as OCMF, aims to achieve two objectives simultaneously. Firstly, it aims to minimize the operational cost of the charging pools, as presented in Eq. (14). Secondly, it aims to maximize the flexibility of the chargers' power.

The base definitions of the charger flexibility for G2V charging strategies were proposed in [41] as follows:

- Upward flexibility: This refers to the power increase a charger can deviate from the nominal dispatched power, reducing the charging time of the EV.
- Downward flexibility: This refers to the power reduction a charger can deviate from the nominal dispatched power. This flexibility can be utilized up to a later time slot when the EV needs to be charged to achieve the required SoC by its departure time.

Then, the G2V upward $F_{i,k}^{cu}$ and downward $F_{i,k}^{cd}$ flexibilities that each EV charger can provide are depicted in Fig. 3. Then, we propose to define the charging flexibility $F_{i,k}^c$ as the minimum flexibility between upward and downward, as,

$$F_{i,k}^c = \min\{F_{i,k}^{cu},\ F_{i,k}^{cd}\}, \tag{16}$$

In line with the charging flexibility discussed earlier, we introduce a discharging V2G flexibility $F_{i,k}^d$, designed to adjust the discharging power either upwards or downwards as needed by the CPO. Thus, to maximize both the upward $F_{i,k}^{du}$ and downward $F_{i,k}^{dd}$ discharging flexibilities, we consider the minimum of both as,

$$F_{i,k}^d = \min\{F_{i,k}^{du},\ F_{i,k}^{dd}\}, \tag{17}$$

Note that only one of the charging or discharging flexibilities can be offered at each sample time when the EV is either charging or discharging. However, when the charger power is zero, both the charging and discharging flexibilities are available (refer to Fig. 3). Furthermore, flexibility is not available after the time d_m as the EV must be charged to reach the EV owner's requested SoC upon departure.

Therefore, the second objective of the OCMF, which aims to maximize the chargers' flexibility, is formulated as follows:

$$O_k^{FM} = \pi_{k,\text{Flex}}^c \sum_{i=1}^{I} F_{i,k}^c + \pi_{k,\text{Flex}}^d \sum_{i=1}^{I} F_{i,k}^d, \tag{18}$$

where, the $\pi_{k,\text{Flex}}^c$ and $\pi_{k,\text{Flex}}^d$ are the incentive prices for offering flexibility.

The EV CPO addresses the following OCMF V2G problem:

$$\min\ \Delta t \sum_{k=0}^{H-1} \left(O_k^{CM} - O_k^{FM}\right) \tag{19a}$$

$$\begin{aligned} \text{s.t. Eqs. (4), (10), (11), (13)} \\ F_{i,k}^c \leq P_{i,k}^c \leq \left(\overline{P}_i^c - F_{i,k}^c\right) z_{i,k} \\ F_{i,k}^d \leq P_{i,k}^d \leq \left(\overline{P}_i^d - F_{i,k}^d\right) (1 - z_{i,k}) \\ 0 \leq F_{i,k}^c \leq \overline{P}_i^c \\ 0 \leq F_{i,k}^d \leq \overline{P}_i^d \\ \forall\ k=1,2,\ldots,H,\ i=1,2,\ldots,I, \\ j=1,2,\ldots,J,\ g=1,2,\ldots,G. \end{aligned} \tag{19b}$$

The decision variables of this problem are the charging $P_{i,k}^c$ and discharging $P_{i,k}^d$ power, the binary variable $z_{i,k}$, and the charging $F_{i,k}^c$ and discharging $F_{i,k}^d$ flexibilities. The charging and discharging powers are constrained by the charger flexibility, with the charging and discharging flexibilities restricted to positive values and bounded between zero and the maximum power.

Notice that as in the eMPC problem, this OCMF problem also applies to the G2V strategy, with the difference being the absence of the

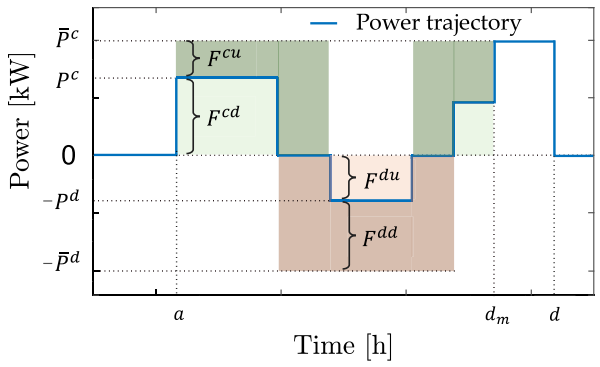

Fig. 3. Flexibility in an EV charger, considering G2V and V2G strategies.

Algorithm 1 Simulation Example using eMPC V2G

```
1: from EV2Gym.ev2gym_env import EV2Gym
2: from ocmf_mpc import OCMF_V2G, OCMF_G2V
3: from eMPC import eMPC_V2G, eMPC_G2V
4: config_file = "config.yaml"                    ▷ Configuration file path
5: env = EV2Gym(config_file)                      ▷ Initialize simulation
6: s_0 = env.reset()
7: agent = eMPC_V2G(env, control_horizon=H)
8: for k in 0, 1, ..., K do
9:     a_{1,...,I} = agent.get_action(s_k)        ▷ MPC optimization
10:    s_{k+1}, stats = env.step(a_{1,...,I})     ▷ Simulate
11: end for
12: profits, total energy charged, ... = stats
```

remuneration price π^d_k since $P^d_{i,k}$ is always zero, the lack of the price $\pi^d_{k,\text{Flex}}$, the flexibility $F^d_{i,k}$, and the binary variable $z_{i,k}$.

As a final remark, while the SoC dynamics are linear, the overall formulation is a MILP due to binary variables enforcing mutually exclusive charging/discharging actions (see Eqs. (15b) and (19b)). The resulting combinatorial structure, efficiently solvable by modern MILP solvers, is naturally integrated within the MPC framework, enabling adaptive, real-time control based on updated forecasts and system states, key features for V2G energy management.

4. Experimental setup

In this section, we describe how to integrate the execution of an EV2Gym [43] simulation, introduced in Section 2, with the proposed MPC algorithms. Alg. 1 outlines the Python code necessary to run a simulation utilizing the `eMPC_V2G` strategy. Initially, the simulator class `EV2Gym` (line 1) and the developed MPC classes `OCMF_V2G`, `OCMF_G2V`, `eMPC_V2G`, and `eMPC_G2V` (lines 2 and 3) are imported. Lines 5 and 6 initialize the simulation environment using a user-defined configuration file (`config_file`). Subsequently, the MPC algorithm's variables are set up in line 7, allowing users to customize the control horizon H as needed. The MPC algorithms are implemented using the Gurobi solver.

The main simulation loop, spanning K steps, commences thereafter. Firstly, charging and discharging actions $\boldsymbol{a}_{1,\dots,I}$ for each charging station $i \in I$ are determined by executing the MPC algorithm's optimization process (line 9), using the current state ($\boldsymbol{s}_k$) of the simulation as input. The state $\boldsymbol{s}_k$ includes essential information such as EVs' SoC, time of arrival and departure, load and PV forecasts, facilitating the decision-making algorithm's optimization. The actions vector $\boldsymbol{a}1, \dots, I$ is constrained within the $[-1, 1]^I$ interval, where -1 denotes maximum power discharge, 1 signifies maximum power charging, and 0 indicates no action. Subsequently, a simulation step is taken (`env.step()`) utilizing the action vector $\mathbf{a}1, \dots, I$ as a parameter (line 10). Each step yields the subsequent simulation state $\boldsymbol{s}_{k+1}$, while the final step ($k = K$) also provides simulation evaluation statistics (`stats`) such as total profits (€), total energy charged and discharged (kWh), execution time (s), and total battery degradation (line 12). These metrics are important for evaluating the efficacy of smart charging algorithms.

Table 3
General simulation parameters.

Name	Symbol	Value
Sample time [min]	Δt	15
Operation time of the station [h]	T	24
Prediction horizon (2.5 h–10 h)	H	$\{2.5 \times 4, 10 \times 4\}$
Number of EVSEs	I	{5–50}
Number of EVs	J	{15–120}
Number of transformers	G	{1, 3}
Discharge price multiplier	m	{0.8–1.2}
EV scenario		"Residential"

4.1. Experimental configuration

The EV2Gym simulator allows for complete configuration of the dynamics of the simulation by modifying the configuration file. Table 3 showcases the general simulation parameters and the values used for the experiments, while Fig. 1 visualizes the experimental setup comprised of EVs, EVSEs, and transformers, inflexible loads, PVs, etc. Specifically, each simulation lasts 24 h, with discrete time steps set at 15 min. Each simulation contains the connection of 5 to 60 EVSEs to either 1 or 3 transformers, accommodating a fleet size ranging from 15 to 120 EVs, as determined by the experimental setups. The EVs' time of arrival, time of departure, and arrival SoC are based on residential EV transaction data from ElaadNL [36]. Also, the discharge price is based on the charge price and multiplier m, thus $\pi^d_k = m \cdot \pi^c_k$. The charging prices used in these simulations are based on the historic Dutch day-ahead prices [44].

Furthermore, the default model parameters, such as transformer power limit, EVSE, and EV characteristics, can be found in Table 4. Specifically, the transformer power limit of 400 kW reflects typical values found in low-voltage distribution networks in residential areas, while the EV battery capacity of 50 kWh corresponds to the median capacity of commercially available EV models in Europe [36]. The simulator also provides forecasts of the loads using a Gaussian distribution ($\bar{l}_{g,k} = \mathcal{N}(\mu, \sigma)$) with mean the $\mu = 100\% \times l_{g,k}$ of the actual load at time k and standard deviation $\sigma = 5\% \times l_{g,k}$ of it. Similarly, for PV generation forecasts $\bar{w}_{g,k}$. Moreover, tool users have the flexibility to customize demand response events by specifying parameters such as the number of events, capacity reduction, duration, and notification time. The start time of events follows a Gaussian distribution with a mean of 18:00 and a standard deviation of 1 h.

5. Experimental results

In this section, a thorough experimental assessment of the proposed MPC strategies is presented. Initially, a detailed examination of a single case study is visualized to understand the behavior of each baseline charging algorithm. Subsequently, the scope is extended by conducting multiple simulations to show average performance, facilitating a comparative analysis across the main evaluation metrics including profitability, flexibility, and battery degradation. Finally, an evaluation of the computational costs associated with the proposed methods is conducted, thereby providing a holistic perspective on their efficacy.

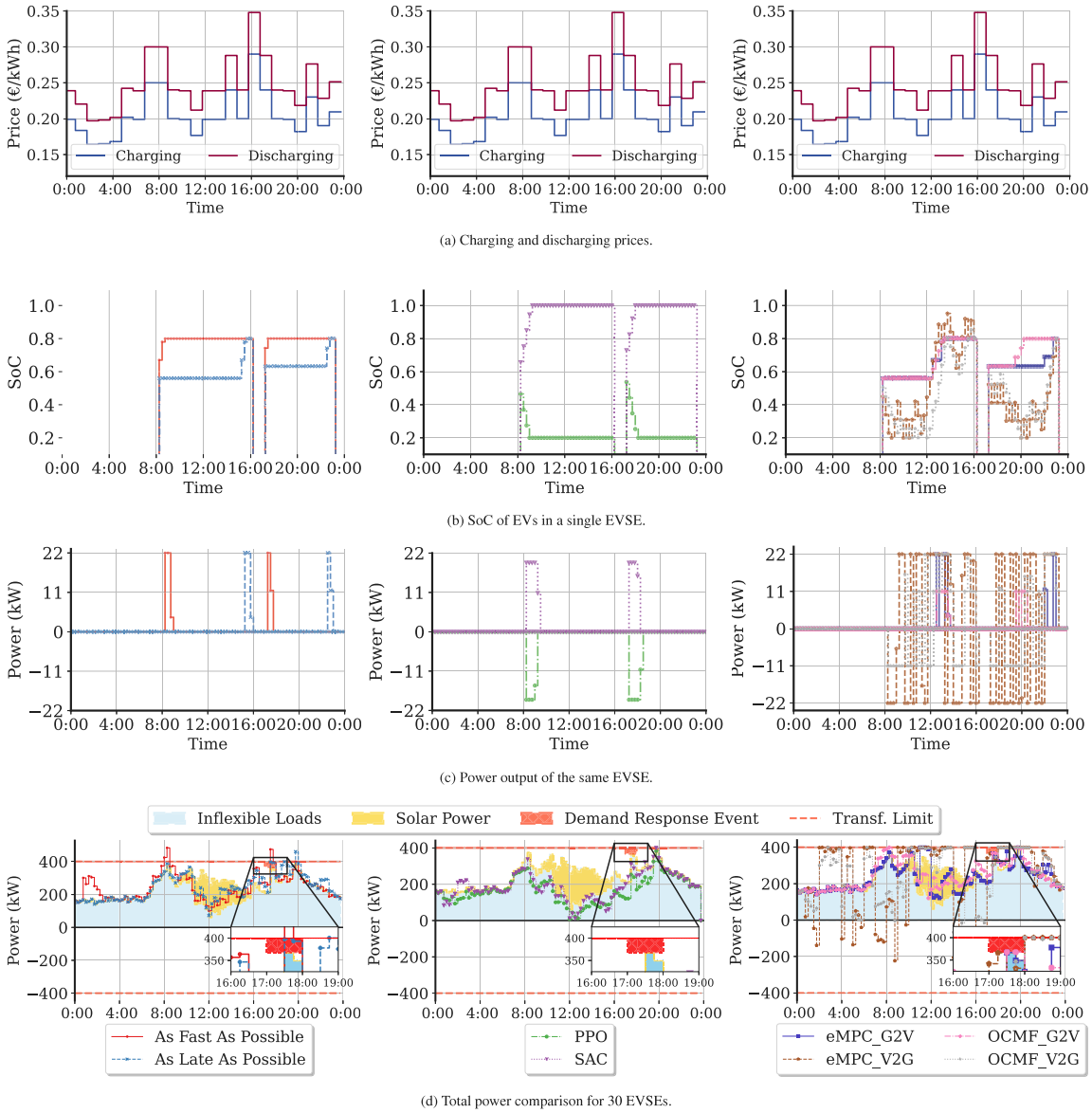

(a) Charging and discharging prices.

(b) SoC of EVs in a single EVSE.

(c) Power output of the same EVSE.

(d) Total power comparison for 30 EVSEs.

Fig. 4. Comparison of baselines, including rule-based and RL algorithms, and the proposed MPC approaches for a case study with 30 EVSEs connected to a single transformer, and around 75 EVs. The zoomed box highlights how MPC respects the demand response event power limit while rule-based algorithms fail.

Table 4
Default simulation model parameters.

Name	Symbol	Value
Transformer power limit [kW]	Ψ	400
Maximum EVSE output power [kW]	$\overline{P}^c$, $\overline{P}^d$	22
EVSE voltage (V)	V	230
EVSE phases	ϕ	3
EV battery capacity [kWh]	E_j	50
Maximum EV power [kW]	$\overline{P}^c$, $\overline{P}^d$	22
Minimum EV SoC when discharging	SoC_j, min	10%
Minimum EV SoC at departure	$\underline{\text{SoC}}_j, d_j$	80%
Minimum EV time of connection [h]		3
Charging efficiency	η^c	100%
Discharging efficiency	η^d	100%
Load and PV forecast error	–	5%
DR capacity reduction	–	20%
DR event duration [h]	–	1
DR event start time [h]	–	18 ± 1

5.1. Baseline charging algorithms

In this study, multiple baselines are compared with the proposed MPC algorithms. Initially, two simpler rule-based algorithms are used: the *charge as fast as possible* strategy (AFAP), and *charge as late as possible* strategy (ALAP). As their name suggests, AFAP fully charges the EVs to their desired capacity as soon as they connect, while ALAP waits to start charging right before the EV leaves (still charging up to desired SoC). Moreover, two state-of-the-art RL algorithms are implemented, the Soft Actor Critic (SAC) and Proximal Policy Optimization (PPO). The RL algorithms are trained using default parameters as described in [43].

5.2. Single case study comparison

To evaluate the proposed MPC methods, their performance was compared against baseline strategies within a single case study. In Fig. 4(d), a detailed comparison is provided between the rule-based strategies (AFAP and ALAP), RL baselines (PPO and SAC), and the

Table 5
Averages of 50 runs with 10 EVSEs, 25 EVs, 1 transformer, and varying EV behavior.

	Algorithm	Profits (€)	User satisfaction (%)	Charged energy (kWh)	Discharged energy (kWh)	$\sum Q^{\text{lost}}$ ($\times 10^{-4}$)	$\sum d^{cal}$ ($\times 10^{-4}$)	$\sum d^{cyc}$ ($\times 10^{-4}$)
Rule based	AFAP	−47.6 ± 8.4	100.0 ± 0.0	227 ± 38	–	12.4 ± 1.6	3.5 ± 0.2	8.8 ± 1.5
	ALAP	−46 ± 11	100.0 ± 0.0	227 ± 38	–	12.2 ± 2.2	2.8 ± 0.4	9.4 ± 2.0
RL	PPO	15 ± 3	59.0 ± 5.9	3 ± 1	61 ± 11	8.7 ± 1.3	2.7 ± 0.4	6.0 ± 1.1
	SAC	−3 ± 12	62.3 ± 1.3	186 ± 42	138 ± 28	15.8 ± 2.3	2.8 ± 0.4	13.0 ± 2.0
MPC	OCMF G2V	−48.0 ± 8.3	100.0 ± 0.0	227 ± 38	–	12.8 ± 1.6	3.3 ± 0.2	9.5 ± 1.5
	OCMF V2G	11.9 ± 8.8	100.0 ± 0.0	927 ± 73	706 ± 63	36.8 ± 2.7	3.1 ± 0.2	33.7 ± 2.5
	eMPC G2V	−43.9 ± 7.6	100.0 ± 0.0	227 ± 38	–	13.3 ± 1.7	3.3 ± 0.2	10.0 ± 1.6
	eMPC V2G	50.8 ± 10.3	100.0 ± 0.0	1390 ± 119	1172 ± 107	57.1 ± 4.8	3.2 ± 0.2	53.9 ± 4.5

MPC variants with a prediction horizon of 10 h ($H = 40$). The evaluation was conducted across four key dimensions: pricing dynamics, EV SoC, power output at the charging station level, and aggregated transformer-level power flow.

Fig. 4(a) depicts the charging and discharging prices observed during the simulation day, with slightly elevated discharging prices to encourage V2G operations. In Fig. 4(b), the SoC evolution of EVs connected to a single EVSE is illustrated, where distinct charging patterns are observed, highlighting the profit-oriented behavior of eMPC and the flexibility-driven behavior of OCMF. The corresponding power output profile of the same EVSE is shown in Fig. 4(c), where the eMPC strategy consistently reaches the maximum power capacity (22 kW), whereas OCMF typically operates at around 11 kW, reflecting its objective to enhance flexibility. As illustrated, the RL method fails to solve the optimal EV-charging problem efficiently, as it prioritizes discharging to maximize profit but misses the target SoC by departure. Finally, the aggregated power output of approximately 75 EVs connected to 30 EVSEs over the course of a day is shown in Fig. 4(d). This analysis includes inflexible loads, PV generation, and a demand response event. It can be observed that both rule-based and RL baselines lead to potential transformer overloads due to the lack of explicit constraint enforcement. In contrast, the proposed MPC methods successfully maintain transformer loading within safe operational limits by optimally managing power limits.

5.3. Performance analysis

In the previous section, the performance was shown for a single case study. However, a comprehensive assessment is necessary across various scenarios. Table 5 presents the mean and standard deviation derived from 50 statistical runs across a configuration comprising 10 bidirectional chargers linked to one transformer, around 25 EVs per simulation, and discharge price multiplier $m = 1.2$. These case studies included elements such as inflexible loads, PV generation, and demand response events, thereby mirroring real-world optimization challenges. Across all scenarios, the MPC methods employed a 10-step prediction horizon (i.e., 2.5 h, $H = 10$) to drive their decision-making processes.

Table 5 illustrates that across all G2V approaches (AFAP, ALAP, OCMF G2V, and eMPC G2V), the average energy consumption remains consistent at approximately 227 ± 38 kWh. Among these, OCMF G2V stands out for its consistent ability to maximize flexibility, enabling rapid responses to demand response events. In contrast, eMPC G2V demonstrates superior cost efficiency, reducing average charging expenses from €48 to €43.9. While the direct cost savings of eMPC G2V over OCMF G2V are modest (around €4), the trade-off highlights the strategic value of OCMF G2V in delivering system-level flexibility, which is often prioritized in grid-support scenarios. When V2G capabilities are enabled, both OCMF V2G and eMPC V2G achieve notable profitability, yielding average profits of approximately €11.9 and €50.8, respectively. These results underscore the potential of V2G strategies not only to support the grid but also to generate meaningful economic returns. By contrast, RL methods achieve comparatively lower charging costs; however, this is accompanied by reduced user satisfaction. Specifically, RL policies often fail to enforce hard constraints such as ensuring full battery charge upon vehicle departure. As highlighted in prior studies, RL requires meticulous reward shaping, constraint handling, and extensive hyperparameter tuning to perform reliably in practical settings. This sensitivity limits its out-of-the-box applicability in real-world deployments without additional methodological safeguards.

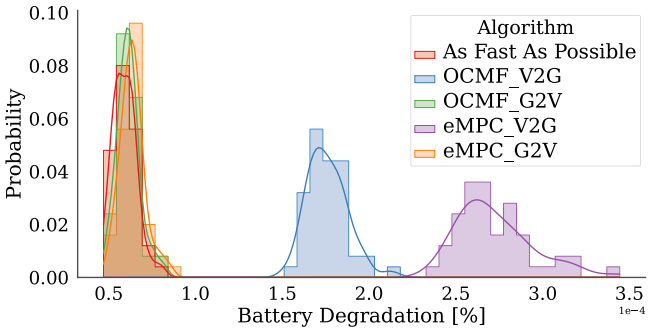

Fig. 5. Histogram of average battery capacity loss per EV after one day for five charging methods; the x-axis shows percent loss and the y-axis its chance, with colors matching the legend.

Moreover, it is crucial to evaluate the impact of the methods on total battery degradation. Table 5 provides insights into the total battery capacity lost (Q^{lost}) during the simulation for all EVs, split into calendar aging (d^{cal}) and cyclic degradation (d^{cyc}) components, while Fig. 5 presents histograms of the average percentage capacity loss per EV ($10^{-4} \times 100\%$) for the best-performing algorithms. RL and the rule-based ALAP methods are excluded from this analysis due to their suboptimal performance in earlier evaluations. Remarkably, V2G methods tend to mitigate calendar aging due to their maintenance of a lower average SoC during the charging phase. However, this advantage is counterbalanced by substantially higher cyclic degradation values (up to 45×10^{-4} higher), stemming from their utilization of EV batteries for both charging and discharging, totaling 2562 kWh—2335 kWh more than G2V methods. Conversely, all G2V methods display comparable battery degradation ($\approx 13 \times 10^{-4}$), with OCMF G2V offering maximal flexibility and eMPC G2V focusing on minimizing charging costs. Overall, these findings underscore the capabilities of the proposed algorithms and their intricate trade-offs among profits, flexibility, and battery degradation.

5.4. Cost sensitivity analysis

In the previous experiments, it was observed that V2G methods can yield profits when the discharge price multiplier is set to $m = 1.2$; however, a sensitivity analysis under alternative pricing scenarios is needed to assess the robustness of this result. In each scenario, the price is defined as:

$$\pi_k^d = m \cdot \pi_k^c, \tag{20}$$

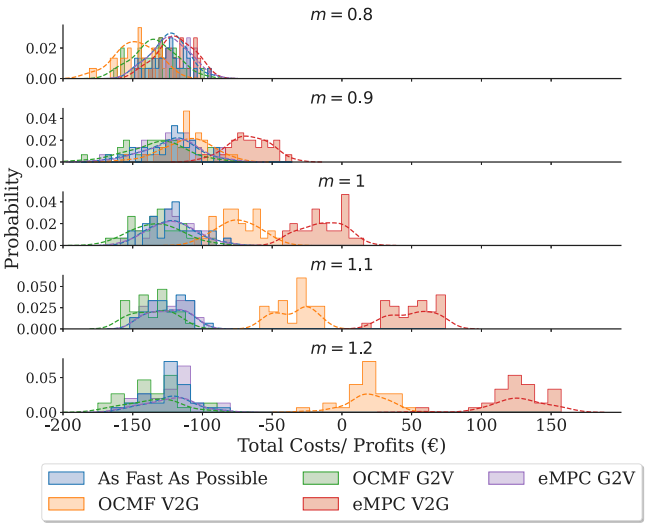

Fig. 6. Comparison of EV-user charging costs across different discharge price multipliers (m). Note that these figures solely reflect EV-user payments. However, it is important to acknowledge that potential profits from flexibility provision are not included here, which could significantly boost overall profits.

for $k = 1, \ldots, T$. Fig. 6 illustrates the probability density functions of the total costs and profits for 50 statistical runs for each price scenario. In every scenario, the G2V and AFAP methods have the same distribution since they are not affected by the discharging prices. As observed in Fig. 6, the eMPC_V2G strategy always provides the highest cost reductions ($m = 0.8, 0.9$) and the highest profits ($m = 1, 1.1, 1.2$). OCMF_V2G is also profitable in all cases except $m = 0.8$, showcasing on average around € 10 higher charging costs; this happens because the cost of providing flexibility was less than discharging, hence leading to this behavior. Notice that in this cost/profit analysis of the OCMF strategy, the payments for flexibility have not been included. Additionally, the costs or profits are considered from the side of the CPO; hence, the costs of individual EV owners are not evaluated and are considered out-of-scope in this study. Therefore, it can be inferred that this strategy would significantly increase its profits when the flexibility offered and provided is considered.

5.5. Computational cost

The proposed MPC methods are designed to efficiently address real-time EV smart-charging challenges. However, it should be noted that execution time increases as the number of decision variables and constraints grows. To evaluate the computational performance of each method, execution times were measured using a high-performance hardware configuration. Specifically, an "AMD RYZEN 7 5700X 8-Core" processor with 32 GB of RAM was employed, along with the Gurobi 11 solver. Fig. 7 presents a comparison of the average per-step execution times across multiple case studies, involving scenarios with 5 to 60 EVSEs connected to three transformers. The reported execution time includes all computational steps for the MPC algorithms: matrix construction, model formulation with constraints, and solution of the optimization problem, with the MIP gap parameter set to zero,[2] while it only includes the inference time of RL algorithms, as training the RL models is performed offline only once. As shown in Fig. 7(a), a gradual increase in per-step execution time is observed when a 10-step prediction horizon is used. In contrast, Fig. 7(b) reveals a more pronounced growth in execution time for a 30-step prediction horizon. As expected, the OCMF V2G method exhibits the largest increase in computational time across both scenarios, due to its higher number of decision variables. Importantly, the G2V variants demonstrate slower scaling behavior, requiring approximately half the execution time of their V2G counterparts. Even in the worst-case scenario, the execution time of the MPC algorithm remains below 1.5% of the control strategy's time step, indicating sufficient space for real-time deployment with larger EVSE fleets. Additionally, note that for the tested scenarios ranging up to 60 EVSEs, only a few (2–3) gigabytes of memory are required, indicating that memory is not a limiting factor at this scale. However, we acknowledge that for significantly larger systems, memory usage may become more critical, and this is highlighted as a consideration for future scalability assessments.

6. Conclusions

In this paper, four model predictive control variants were developed and tested for real-time smart charging of EV in both G2V and V2G modes. These controllers incorporated transformer capacity constraints, demand response events, and dynamic electricity pricing. The open-source implementation was evaluated extensively in scenarios with up to thirty EVSE. The results showed that the proposed model predictive control methods significantly reduced violations of transformer power limits and provided improved economic performance compared to rule-based and RL approaches. Furthermore, a comprehensive analysis of battery degradation indicated that the V2G-enabled controllers consistently maintained daily capacity loss below 0.005%, while achieving a balance between operational flexibility and profitability. These findings demonstrated the practicality and scalability of the proposed approach for real-world deployment in distributed electric vehicle charging systems.

Future work could integrate battery degradation directly into the MPC model to balance short-term profit and long-term battery health. Evaluating the framework in other settings, such as DC fast chargers, workplaces, or public infrastructure, would test its generalizability and real-time performance under different conditions. Additionally, analyzing the charging process from the user's perspective, including costs, incentives, and behavior, would enable more personalized and economically transparent strategies. Moreover, while existing open-source platforms for EV aggregation in V2X applications provide valuable tools, they generally lack integration with region-specific market regulations and power system operator contracts. These regulatory frameworks differ substantially across jurisdictions, such as the US, Canada, the EU, and China, and their impact on aggregation potential, operational constraints, and business models remains insufficiently

[2] Note that increasing the MIP gap can substantially reduce execution time, albeit at the expense of solution quality.

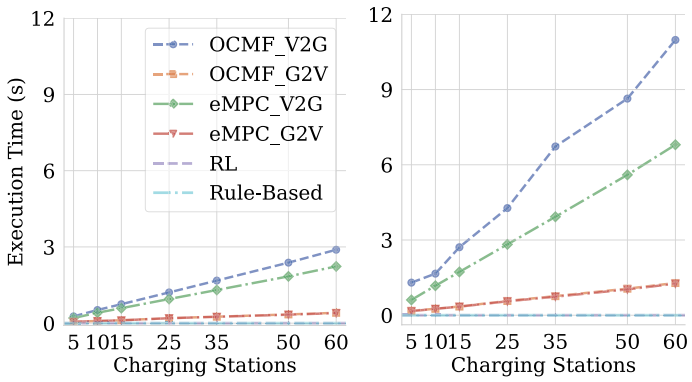

(a) $h = 10$ (b) $h = 30$

Fig. 7. Average step execution time for varying control horizons and EVSEs.

studied. Exploring this regulatory dimension could uncover key limitations and opportunities, making it a promising avenue for future research.

CRediT authorship contribution statement

Cesar Diaz-Londono: Writing – review & editing, Writing – original draft, Software, Methodology, Funding acquisition, Conceptualization. **Stavros Orfanoudakis:** Writing – review & editing, Writing – original draft, Visualization, Methodology, Conceptualization. **Pedro P. Vergara:** Writing – review & editing, Validation, Project administration, Funding acquisition. **Peter Palensky:** Funding acquisition. **Fredy Ruiz:** Writing – review & editing, Conceptualization. **Giambattista Gruosso:** Writing – review & editing, Conceptualization.

Declaration of competing interest

The authors declare that they have no known competing financial interests or personal relationships that could have appeared to influence the work reported in this paper.

Acknowledgments

Cesar was granted by Politecnico di Milano within the IDEA League Alliance through the IDEA League Fellowship Exchange Program 2023. Cesar was funded by FSE-REACT EU, PON “RICERCA e INNOVAZIONE” 2014–2020, Azione IV.6 (Green). Stavros is funded by the HORIZON Europe Drive2X Project 101056934.

Data availability

We made the code open source.

References

[1] K.M. Tan, V.K. Ramachandaramurthy, J.Y. Yong, Integration of electric vehicles in smart grid: A review on vehicle to grid technologies and optimization techniques, Renew. Sustain. Energy Rev. 53 (2016) 720–732.

[2] A. Dubey, S. Santoso, Electric vehicle charging on residential distribution systems: Impacts and mitigations, IEEE Access 3 (2015) 1871–1893.

[3] L. Shi, T. Lv, Y. Wang, Vehicle-to-grid service development logic and management formulation, J. Mod. Power Syst. Clean Energy 7 (4) (2019) 935–947, http://dx.doi.org/10.1007/s40565-018-0464-7.

[4] A. Allehyani, A. Ajabnoor, M. Alharbi, Chapter 14 - demand response scheme for electric vehicles charging in smart power systems with 100% of renewable energy, in: S. Chenniappan, S. Padmanaban, S. Palanisamy (Eds.), Power Systems Operation with 100% Renewable Energy Sources, Elsevier, 2024, pp. 247–268, http://dx.doi.org/10.1016/B978-0-443-15578-9.00016-9.

[5] W. Abdelfattah, A.S. Abdelhamid, H.M. Hasanien, B.A.-E. Rashad, Smart vehicle-to-grid integration strategy for enhancing distribution system performance and electric vehicle profitability, Energy 302 (2024) 131807, http://dx.doi.org/10.1016/j.energy.2024.131807.

[6] A.F. Güven, Integrating electric vehicles into hybrid microgrids: A stochastic approach to future-ready renewable energy solutions and management, Energy 303 (2024) 131968, http://dx.doi.org/10.1016/j.energy.2024.131968.

[7] A. Nouri, A. Lachheb, L. El Amraoui, Optimizing efficiency of vehicle-to-grid system with intelligent management and ANN-PSO algorithm for battery electric vehicles, Electr. Power Syst. Res. 226 (2024) 109936, http://dx.doi.org/10.1016/j.epsr.2023.109936.

[8] G. Srihari, R.S.R. Krishnam Naidu, P. Falkowski-Gilski, P. Bidare Divakarachari, R. Kiran Varma Penmatsa, Integration of electric vehicle into smart grid: a meta heuristic algorithm for energy management between V2G and G2V, Front. Energy Res. Volume 12 - 2024 (2024) http://dx.doi.org/10.3389/fenrg.2024.1357863.

[9] S.A. Finecomess, G. Gebresenbet, W.Y. Zada, Y. Mulugeta, A. Addisie, Optimization of vehicle-to-grid, grid-to-vehicle, and vehicle-to-everything systems using artificial bee colony optimization, Energies 18 (8) (2025) http://dx.doi.org/10.3390/en18082046.

[10] Majed, N.K. Roy, A. Ahmed, Optimizing the load curve through V2G technology for sustainable energy management, Energy Rep. 13 (2025) 5848–5863, http://dx.doi.org/10.1016/j.egyr.2025.04.066.

[11] S. Orfanoudakis, V. Robu, E.M. Salazar Duque, et al., Scalable reinforcement learning for large-scale coordination of electric vehicles using graph neural networks, 2024, Preprint (Version 1) available at Research Square. URL https://doi.org/10.21203/rs.3.rs-5504138/v1. (Accessed 19 December 2024).

[12] S. Orfanoudakis, N.K. Panda, P. Palensky, P.P. Vergara, GNN-DT: Graph neural network enhanced decision transformer for efficient optimization in dynamic environments, 2025, arXiv:2502.01778.

[13] M.N. Boukoberine, M.F. Zia, T. Berghout, M. Benbouzid, Reinforcement learning-based energy management for hybrid electric vehicles: A comprehensive up-to-date review on methods, challenges, and research gaps, Energy AI 21 (2025) 100514, http://dx.doi.org/10.1016/j.egyai.2025.100514.

[14] PRAFT and RPBFT: A class of blockchain consensus algorithm and their applications in electric vehicles charging scenarios for V2G networks, Internet Things Cyber-Phys. Syst. 3 (2023) 61–70, http://dx.doi.org/10.1016/j.iotcps.2023.02.003.

[15] S.H. Shamsdin, A. Seifi, M. Rostami-Shahrbabaki, B. Rahrovi, Plug-in electric vehicle optimization and management charging in a smart parking lot, in: 2019 IEEE Texas Power and Energy Conference, TPEC 2019, Institute of Electrical and Electronics Engineers Inc., 2019, http://dx.doi.org/10.1109/TPEC.2019.8662169.

[16] K. Schulte, J. Haubrock, Linear programming to increase the directly used photovoltaic power for charging several electric vehicles, in: 2021 IEEE Madrid PowerTech, PowerTech 2021 - Conference Proceedings, Institute of Electrical and Electronics Engineers Inc., 2021, http://dx.doi.org/10.1109/POWERTECH46648.2021.9494914.

[17] I. Sengor, O. Erdinc, B. Yener, A. Tascikaraoglu, J.P. Catalao, Optimal energy management of EV parking lots under peak load reduction based DR programs considering uncertainty, IEEE Trans. Sustain. Energy 10 (3) (2019) 1034–1043, http://dx.doi.org/10.1109/TSTE.2018.2859186.

[18] P. Meenakumar, M. Aunedi, G. Strbac, Optimal business case for provision of grid services through EVs with V2G capabilities, in: 2020 15th International Conference on Ecological Vehicles and Renewable Energies, EVER 2020, Institute of Electrical and Electronics Engineers Inc., 2020, http://dx.doi.org/10.1109/EVER48776.2020.9242538.

[19] F. Giordano, C. Diaz-Londono, G. Gruosso, Comprehensive aggregator methodology for EVs in V2G operations and electricity markets, IEEE Open J. Veh. Technol. 4 (2023) 809–819, http://dx.doi.org/10.1109/OJVT.2023.3323087.

[20] X. Jiang, S. Wang, Q. Zhao, X. Wang, Optimized dispatching method for flexibility improvement of AC-MTDC distribution systems considering aggregated electric vehicles, J. Mod. Power Syst. Clean Energy 11 (6) (2023) 1857–1867, http://dx.doi.org/10.35833/MPCE.2022.000576.

[21] H. Patil, V.N. Kalkhambkar, Grid integration of electric vehicles for economic benefits: A review, J. Mod. Power Syst. Clean Energy 9 (1) (2021) 13–26, http://dx.doi.org/10.35833/MPCE.2019.000326.

[22] J.S. Giraldo, N.B. Arias, P.P. Vergara, M. Vlasiou, G. Hoogsteen, J.L. Hurink, Estimating risk-aware flexibility areas for electric vehicle charging pools via AC stochastic optimal power flow, J. Mod. Power Syst. Clean Energy 11 (4) (2023) 1247–1256, http://dx.doi.org/10.35833/MPCE.2022.000452.

[23] C. Diaz-Londono, G. Fambri, P. Maffezzoni, G. Gruosso, Enhanced EV charging algorithm considering data-driven workplace chargers categorization with multiple vehicle types, eTransportation 20 (2024) 100326, http://dx.doi.org/10.1016/j.etran.2024.100326.

[24] M. Tahmasebi, A. Ghadiri, M. Haghifam, S. Miri-Larimi, MPC-based approach for online coordination of EVs considering EV usage uncertainty, Int. J. Electr. Power Energy Syst. 130 (2021) 106931.

[25] Z. Ji, X. Huang, C. Xu, H. Sun, Accelerated model predictive control for electric vehicle integrated microgrid energy management: A hybrid robust and stochastic approach, Energies 9 (11) (2016) http://dx.doi.org/10.3390/en9110973.

[26] Y. Zhou, A. Ravey, M.-C. Péra, Real-time cost-minimization power-allocating strategy via model predictive control for fuel cell hybrid electric vehicles, Energy Convers. Manage. 229 (2021) 113721, http://dx.doi.org/10.1016/j.enconman.2020.113721.

[27] C. Minchala-Ávila, P. Arévalo, D. Ochoa-Correa, A systematic review of model predictive control for robust and efficient energy management in electric vehicle integration and V2G applications, Modelling 6 (1) (2025) http://dx.doi.org/10.3390/modelling6010020.

[28] J.R.A. Klemets, E. Haugen, B.N. Torsæter, MPC-based control structure for high-power charging stations capable of providing ancillary services, Int. J. Electr. Power Energy Syst. 159 (2024) 110039, http://dx.doi.org/10.1016/j.ijepes.2024.110039.

[29] E. Cording, J. Thakur, FleetRL: Realistic reinforcement learning environments for commercial vehicle fleets, SoftwareX 26 (2024) 101671, http://dx.doi.org/10.1016/j.softx.2024.101671.

[30] G. Karatzinis, C. Korkas, M. Terzopoulos, C. Tsaknakis, A. Stefanopoulou, I. Michailidis, E. Kosmatopoulos, Chargym: An EV charging station model for controller benchmarking, in: Artificial Intelligence Applications and Innovations, Springer International Publishing, 2022, pp. 241–252.

[31] C. Yeh, V. Li, R. Datta, J. Arroyo, N. Christianson, C. Zhang, Y. Chen, M.M. Hosseini, A. Golmohammadi, Y. Shi, Y. Yue, A. Wierman, SustainGym: Reinforcement learning environments for sustainable energy systems, 2023.

[32] T. Morstyn, K.A. Collett, A. Vijay, M. Deakin, S. Wheeler, S.M. Bhagavathy, F. Fele, M.D. McCulloch, OPEN: An open-source platform for developing smart local energy system applications, Appl. Energy 275 (2020) 115397, http://dx.doi.org/10.1016/j.apenergy.2020.115397, URL https://www.sciencedirect.com/science/article/pii/S0306261920309090.

[33] C. Dalamagkas, V. Melissianos, G. Papadakis, A. Georgakis, V.-M. Nikiforidis, K. Hrissagis-Chrysagis, The open V2X management platform: An intelligent charging station management system, Inf. Syst. 129 (2025) 102494, http://dx.doi.org/10.1016/j.is.2024.102494.

[34] T. Qian, M. Fang, Q. Hu, C. Shao, J. Zheng, V2sim: An open-source microscopic V2G simulation platform in urban power and transportation network, IEEE Trans. Smart Grid (2025) http://dx.doi.org/10.1109/TSG.2025.3560976, 1–1.

[35] O. Frendo, N. Gaertner, H. Stuckenschmidt, Open source algorithm for smart charging of electric vehicle fleets, IEEE Trans. Ind. Inform. 17 (9) (2021) 6014–6022, http://dx.doi.org/10.1109/TII.2020.3038144.

[36] Elaadnl open datasets for electric mobility research | update april 2020, 2023, https://platform.elaad.io/analyses/ElaadNL_opendata.php. (Accessed 23 November 2023).

[37] Pecan Street Data Portal. https://www.pecanstreet.org/dataport/.

[38] S. Pfenninger, I. Staffell, Long-term patterns of European PV output using 30 years of validated hourly reanalysis and satellite data, Energy 114 (2016) 1251–1265.

[39] A.A.E. Elsayed, S. Saxena, H.E.Z. Farag, Optimal design of a planning and contracting framework to enable vehicle to building and grid services via demand response, IEEE Trans. Transp. Electrification 11 (3) (2025) 7542–7556, http://dx.doi.org/10.1109/TTE.2025.3529346.

[40] C.F. Lee, K. Bjurek, V. Hagman, Y. Li, C. Zou, Vehicle-to-grid optimization considering battery aging, 22nd IFAC World Congr. 56 (2) (2023) 6624–6629.

[41] C. Diaz-Londono, P. Maffezzoni, L. Daniel, G. Gruosso, Comparison and analysis of algorithms for coordinated EV charging to reduce power grid impact, IEEE Open J. Veh. Technol. 5 (2024) 990–1003, http://dx.doi.org/10.1109/OJVT.2024.3435489.

[42] C. Diaz, F. Ruiz, D. Patino, Smart charge of an electric vehicles station: A model predictive control approach, in: 2018 IEEE Conference on Control Technology and Applications, CCTA, 2018, pp. 54–59, http://dx.doi.org/10.1109/CCTA.2018.8511498.

[43] S. Orfanoudakis, C. Diaz-Londono, Y. Emre Yılmaz, P. Palensky, P.P. Vergara, EV2gym: A flexible V2G simulator for EV smart charging research and benchmarking, IEEE Trans. Intell. Transp. Syst. 26 (2) (2025) 2410–2421, http://dx.doi.org/10.1109/TITS.2024.3510945.

[44] ENTSO-E transparency platform. https://transparency.entsoe.eu/.